Geophysical Prospecting, 2009, **57**, 61–74 doi:10.1111/j.1365-2478.2008.00721.x

Effects of uncertainty in rock-physics models on reservoir parameter estimation using seismic amplitude variation with angle and controlled-source electromagnetics data

Jinsong Chen[1]* and Thomas A. Dickens[2]

[1]*Lawrence Berkeley National Laboratory, Department of Geophysics, 1 Cyclotron Road, Berkeley CA 94720, USA, and* [2]*ExxonMobil Upstream Research Company, Greenway Plaze 3, URC-GW30926, Houston TX 77252–2189, USA*

Received September 2007, revision accepted March 2008

ABSTRACT

This paper investigates the effects of uncertainty in rock-physics models on reservoir parameter estimation using seismic amplitude variation with angle and controlled-source electromagnetics data. The reservoir parameters are related to electrical resistivity by the Poupon model and to elastic moduli and density by the Xu-White model. To handle uncertainty in the rock-physics models, we consider their outputs to be random functions with modes or means given by the predictions of those rock-physics models and we consider the parameters of the rock-physics models to be random variables defined by specified probability distributions. Using a Bayesian framework and Markov Chain Monte Carlo sampling methods, we are able to obtain estimates of reservoir parameters and information on the uncertainty in the estimation. The developed method is applied to a synthetic case study based on a layered reservoir model and the results show that uncertainty in both rock-physics models and in their parameters may have significant effects on reservoir parameter estimation. When the biases in rock-physics models and in their associated parameters are unknown, conventional joint inversion approaches, which consider rock-physics models as deterministic functions and the model parameters as fixed values, may produce misleading results. The developed stochastic method in this study provides an integrated approach for quantifying how uncertainty and biases in rock-physics models and in their associated parameters affect the estimates of reservoir parameters and therefore is a more robust method for reservoir parameter estimation.

INTRODUCTION

Rock-physics models are needed for reservoir parameter estimation using seismic amplitude variation with angle (AVA) and controlled-source electromagnetics (CSEM) data. In practice, these models are often derived from suitable nearby borehole logs. Firstly, appropriate families of rock-physics models are chosen. For instance, we may choose a sand-clay model by Dvorkin and Nur (1996), the Xu-White model by Xu and White (1995) or a differential effective medium model by Norris (1985) and Mavko, Mukerji and Dvorkin (1998) for seismic AVA data and we may choose Archie's law (Archie 1942) or the Poupon model (Poupon, Loy and Tixier 1954; Poupon and Leveaux 1971) for CSEM data.

Secondly, the parameters in the chosen rock-physics models are estimated by fitting them to the selected borehole logs. Since relationships between the reservoir parameters and the geophysical attributes are often nonlinear and non-unique, the derived rock-physics models are inevitably subject to uncertainty and even unknown biases. These may include uncertainty and biases due to an inappropriate choice of the rock-physics model families and those due to inaccurate estimation of the associated model parameters.

*E-mail: jchen@lbl.gov

Uncertainty in rock-physics models may have significant effects on reservoir parameter estimation from geophysical data, especially when the rock-physics models contain unknown biases. Traditional analyses of the effects of uncertainty in the rock-physics models are performed by varying a small subset (e.g., one or two) of the rock-physics parameters while keeping others unchanged, as performed by Hoversten *et al.* (2006). In essence, those methods explore the marginal effects of the parameters on reservoir parameter estimation and are valid only when the parameters being investigated are independent of those being kept unchanged. Since rock-physics parameters often depend on each other, the utility of such approaches is limited. Additionally, the above methods only analyse the effects of uncertainty in the estimated rock-physics parameters without considering uncertainty in the rock-physics model outputs.

An alternative for studying the effects of uncertainty in rock-physics models is to consider geophysical properties as random functions of reservoir parameters, which follow some probability distributions (e.g., Gaussian distributions), using a Bayesian framework. The rock-physics models derived from borehole logs provide only reference values for the reservoir parameters being estimated. An example of such an approach is given by Bachrach (2006), where sediment bulk and shear moduli and density were considered as random functions of reservoir water saturation and porosity and both parameters were estimated jointly by conditioning on seismic AVA data. The above methods mainly focus on the effect of uncertainty in rock-physics model outputs without considering the effect of uncertainty caused by individual rock-physics parameters. In practice, both uncertainties exist and they may affect the estimates of reservoir parameters differently.

In this study, we choose the Xu-White model to relate reservoir parameters to seismic properties and the Poupon model to relate reservoir parameters to electrical properties. Although the choice of suitable rock-physics models in practice is another source of uncertainty, this study is focused solely on investigations of the effects of uncertainty in the chosen rock-physics models. We develop a Bayesian integrated approach based on a layered reservoir model, similar to the one given by Chen *et al.* (2007), with the addition of stochastic rock-physics models to account for this source of uncertainty. We use Markov Chain Monte Carlo methods to explore the joint posterior probability density function. Bayesian models have also been demonstrated by Malinverno and Griggs (2004) to be effective methods for analysing other types of uncertainty in geophysical inverse problems.

The paper is organized as follows. The second section describes the stochastic rock-physics models used in this study, including the Poupon and the Xu-White models and the third section describes our joint inversion Bayesian model with the stochastic rock-physics models included. The synthetic case studies based on a simplified model of an oil-bearing sand reservoir embedded in a shale section are given in the fourth section and discussion and conclusions are given in the fifth section.

STOCHASTIC ROCK-PHYSICS MODELS

In this section, we describe the rock-physics models used in the joint inversion of seismic AVA and CSEM data. We consider geophysical properties, such as electrical resistivity, elastic bulk and shear moduli and density, as random functions of reservoir parameters, such as porosity, water saturation and shale content and of the parameters associated with the rock-physics models.

Electrical resistivity

We connect electrical resistivity to water saturation, porosity and shale content via the Indonesia formula of the Poupon model (Poupon *et al.* 1954; Poupon and Leveaux 1971). The model is a modification of Archie's law (Archie 1942) that accounts for the effect of shale content and is given by:

$$\frac{S_w^{-m}}{\sqrt{r}} = \frac{\varphi^{0.5n}}{\sqrt{r_b}} + \frac{c^{1-0.5c}}{\sqrt{r_c}}, \tag{1}$$

where r represents electrical resistivity in a given layer, S_w, φ and c represent water saturation, porosity and shale content in the same layer and r_b, r_c, m and n represent brine resistivity, shale resistivity and the exponential components of water saturation and porosity, respectively. The model parameters r_b, r_c, m and n are often estimated from nearby borehole logs and in many cases, the parameters m and n are close to 2 (Mavko *et al.* 1998). Figure 1 shows an example of the relationship between electrical resistivity and water saturation, shale content and porosity when $r_b = 0.16$ Ωm, $r_c = 0.50$ Ωm and $m = n = 2$. This relationship will be used in the synthetic study presented in the fourth section. We can see that electrical resistivity is most sensitive to changes in water saturation and porosity and that it varies by several orders of magnitude when water saturation or porosity is small.

Two types of uncertainty may exist in equation (1). The first type is the uncertainty associated with the model parameters r_b, r_c, m and n. To account for the effects of such uncertainty in joint inversion, we consider these parameters to be random

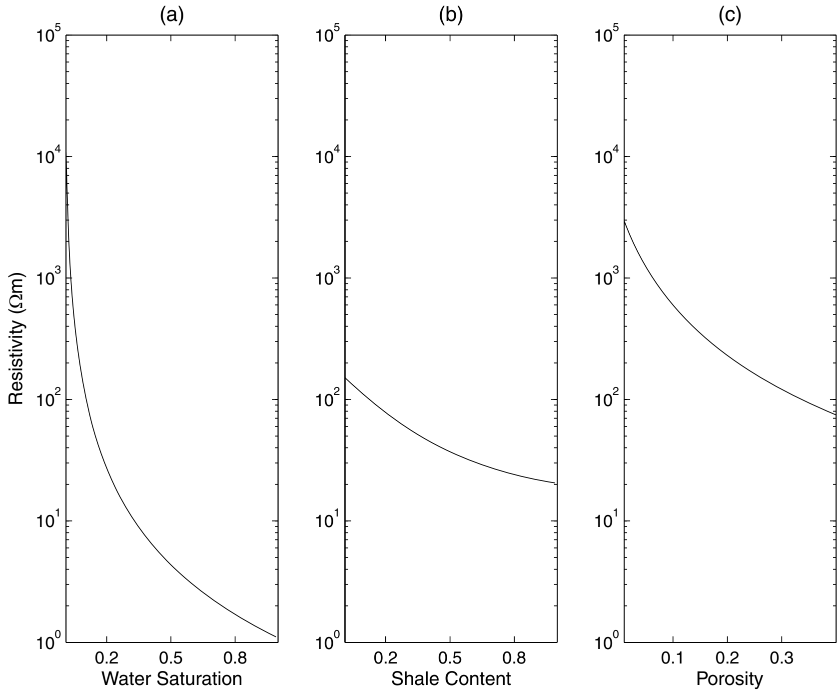

Figure 1 An example showing the relationship between electrical resistivity and water saturation, shale content and porosity, where $r_b = 0.16\ \Omega m$, $r_c = 0.50\ \Omega\text{m}$ and $m = n = 2$. In Fig. 1(a), shale content is 0.1 and porosity is 0.32, in Fig. 1(b), water saturation is 0.1 and porosity is 0.32 and in Fig. 1(c), both shale content and water saturation are 0.1.

variables with given distributions (e.g., uniform or truncated Gaussian distributions). The second type is the uncertainty associated with the output of the Poupon model; for example, this error may arise when the parameterization given in equation (1) cannot accurately describe the measured resistivity. Similarly, to account for the effects of this uncertainty, we consider the predicted resistivity as a random function of water saturation, porosity, shale content and model parameters, defined on the interval of $(0, +\infty)$.

We use a gamma probability distribution with shape parameter α and scale parameter β to describe the uncertainty in the output of the Poupon model. The mean, variance and mode of the gamma distribution are given by $\alpha\beta$, $\alpha\beta^2$ and $\beta(\alpha - 1)$, respectively. Let q be the coefficient of variation of electrical resistivity r, which is defined as the ratio of the standard deviation to the mean and is given by $q = \beta\sqrt{\alpha}/(\alpha\beta) = 1/\sqrt{\alpha}$. Let the mode of the gamma distribution be equal to the electrical resistivity obtained from equation (1). Let $\boldsymbol{\theta}_1 = (r_b, r_c, m, n)^T$, where T represents the transpose of the vector. Consequently, we obtain the conditional probability distribution function of resistivity given the reservoir parameters S_w, φ and c and unknown model parameter $\boldsymbol{\theta}_1$ as follows:

$$f(r \mid S_w, \varphi, c, \boldsymbol{\theta}_1) = \frac{r^{\alpha-1}}{\beta^{\alpha}\Gamma(\alpha)} \exp\left(-\frac{r}{\beta}\right), \tag{2}$$

where $\alpha = 1/q^2$ and $\beta = r_{\text{mode}}\, q^2/(1 - q^2)$. We use the gamma distribution rather than the commonly used log-normal distribution because the gamma distribution provides a more accurate description of errors in electrical resistivity for a given value of the coefficient of variation than does the log-normal distribution (Firth 1988; Cadigan and Myers 2001).

The conditional distribution of electrical resistivity given water saturation, porosity and shale content $f(r \mid S_w, \varphi, c)$, which is used for joint inversion when the model parameters r_b, r_c, m and n are given as fixed values, is different from that when the model parameters are unknown. They are related by:

$$f(r \mid S_w, \varphi, c) = \int f(r \mid S_w, \varphi, c, \boldsymbol{\theta}_1)\, f(\boldsymbol{\theta}_1) d\boldsymbol{\theta}_1, \tag{3}$$

where $f(\boldsymbol{\theta}_1)$ is the probability density function of the unknown model parameter $\boldsymbol{\theta}_1$. When the model parameters are given, the probability density function $f(\boldsymbol{\theta}_1)$ becomes a delta function. Equation (3) suggests that uncertainty in the model parameter $\boldsymbol{\theta}_1$ leads to an increase of uncertainty in the resistivity calculated from equation (1). Figure 2 shows an example of the conditional distribution of electrical resistivity when the model parameters are uncertain and have uniform distributions. The figure depicts quantitatively how the uncertainty in the resistivity predicted by the Poupon model increases as the model parameters become more poorly constrained, given the assumption of gamma-distributed model outputs.

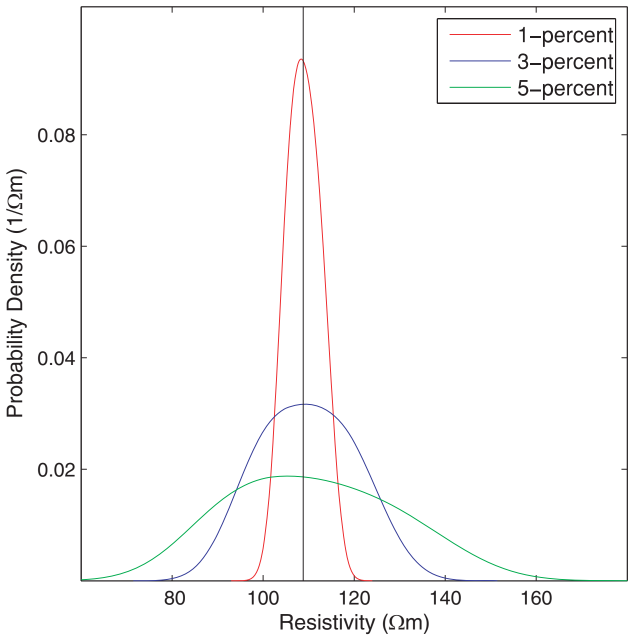

Figure 2 Conditional probability distributions given water saturation (0.1), shale content (0.1) and porosity (0.32) as brine resistivity, shale resistivity and the exponential components of water saturation and porosity in the Poupon model vary uniformly around their corresponding true values, where the red, blue and green curves are the results when the relative errors are 1, 3 and 5%, respectively.

Elastic bulk and shear moduli and density

We relate elastic bulk and shear moduli and density to reservoir parameters using a clay-sand mixture model developed by Xu and White (1995), based on the effective medium theories given by Gassmann (1951) and Kuster and Toksöz (1974). The main feature of the model lies in the assumptions that the total pore space of the medium consists of pores in sand grains and pores in clays and that the pore geometry of sand grains is significantly different from that of clays. As a result, the effect of porosity in shale on elastic properties is very different from the effect of porosity in sandstone. The Xu-White model has been demonstrated to be useful under a wide range of conditions, for example, in formations varying from unconsolidated to consolidated sandstone and shale.

The main parameters associated with the Xu-White model include the bulk and shear moduli and density of sand grains, clay and fluid and the pore aspect ratios of sand and clay. Since the Xu-White model assumes that there are only two phases (i.e., water and either oil or gas), the reservoir parameters that affect reservoir elastic bulk and shear moduli and density are water saturation, clay content and porosity. For ease of description, we use the vector $\boldsymbol{\theta}_2$ to represent all the model parameters and consider them to be random variables in order to account for their uncertainties. The model parameters can be estimated with uncertainty from well log data by adjusting them to provide a good prediction of elastic moduli and density, given porosity, water saturation and shale content. Figure 3 shows the relationship of elastic bulk and shear moduli and density versus water saturation, shale content and porosity using the Xu-White model and parameters given in Table 1. We can see that elastic moduli are most sensitive to changes in porosity and less sensitive to changes in shale content and water saturation, especially when water saturation is small.

To account for the uncertainty in the Xu-White model for a given set of model parameters, we assume that the estimated elastic moduli and density calculated from reservoir parameters using the Xu-White model are distributed according to a multivariate Gaussian distribution with means equal to the outputs of the Xu-White model and a covariance matrix determined from a given correlation structure and coefficients of variation. For the synthetic study presented in the fourth section, we assume that each output of the Xu-White model is independent of the other outputs. For other studies, we can use any desired correlation structure.

Let variables K, μ and ρ represent reservoir elastic bulk and shear moduli and density, respectively. Let ε_K, ε_μ and ε_ρ represent the additive errors in the outputs of the Xu-White model. Let $\mathbf{m}_{rock}$ represent the Xu-White model. Thus,

$$(K, \mu, \rho)^T = \mathbf{m}_{rock}(S_w, \varphi, c, \boldsymbol{\theta}_2) + (\varepsilon_K, \varepsilon_\mu, \varepsilon_\rho)^T. \tag{4}$$

The joint conditional probability density function of the elastic attributes is given by:

$$f(K, \mu, \rho \mid S_w, \varphi, c, \boldsymbol{\theta}_2) = \frac{1}{\sqrt{(2\pi)^3\,|\Sigma|}} \exp\left(-\varepsilon^T \Sigma^{-1} \varepsilon\right), \tag{5}$$

where the symbol $\varepsilon = (\varepsilon_K, \varepsilon_\mu, \varepsilon_\rho)^T$ and the symbol Σ represent the covariance matrix of the error vector ε, which is determined from the given coefficients of variation.

BAYESIAN MODEL

In this section, we extend the Bayesian model developed by Chen *et al.* (2007) for reservoir parameter estimation using seismic amplitude variation with angle (AVA) and controlled-source electromagnetics (CSEM) data. The primary difference between the present study and the one presented by Chen *et al.* (2007) lies in the use of stochastic rock-physics models, where the reservoir geophysical attributes calculated from their corresponding reservoir parameters using rock-physics models

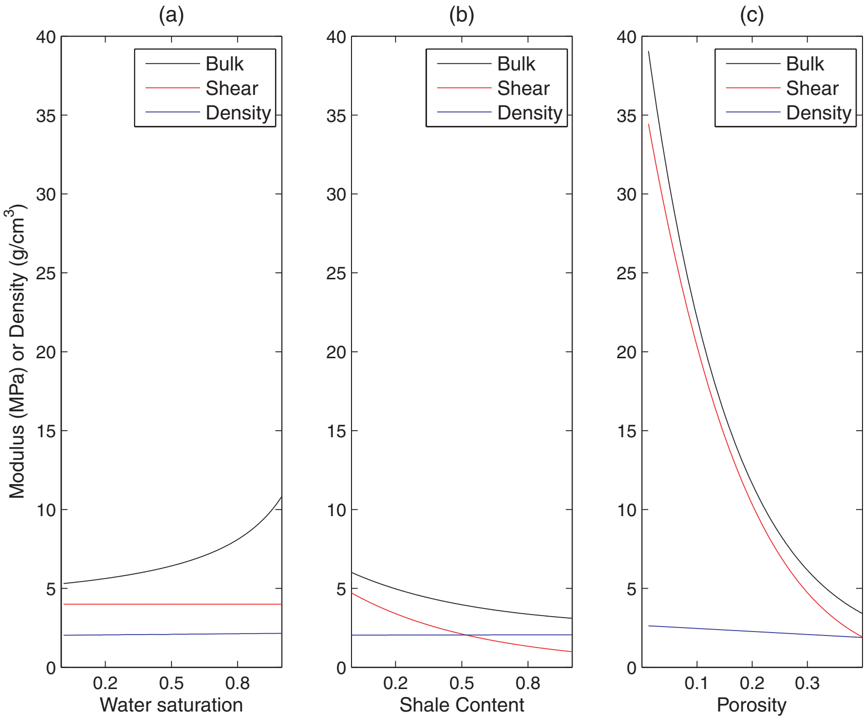

Figure 3 Relationships of elastic moduli and density versus water saturation, shale content and porosity calculated using the Xu-White model and parameters given in Table 1, where shale content is 0.1 and porosity is 0.32 for (a), water saturation is 0.1 and porosity is 0.32 for (b) and both water saturation and shale content are 0.1 for (c).

Table 1 Model parameters in the Xu-White model

Model Parameters	Values
Sand bulk modulus (GPa)	42.584
Sand shear modulus (GPa)	40.470
Sand density (g/cm^3)	2.6500
Sand aspect ratio	0.0900
Clay bulk modulus (GPa)	34.260
Clay shear modulus (GPa)	18.504
Clay density (g/cm^3)	2.6800
Clay aspect ratio	0.0600
Brine bulk modulus (GPa)	3.2200
Brine density (g/cm^3)	1.0900
Oil bulk modulus (GPa)	0.7500
Oil density (g/cm^3)	0.70910

are random functions of the reservoir parameters rather than deterministic values.

Bayesian framework

Figure 4 shows a schematic of a layered marine reservoir with unknown parameters that we wish to estimate. In the target zone (the reservoir layer), we estimate water saturation $\mathbf{S}_w$, porosity φ and shale content **c**. Similar to the model studied by Chen *et al.* (2007), we add several layers above and below the reservoir to account for uncertainty in selecting the time window for seismic AVA data inversion. For those layers, we invert for elastic bulk modulus $\mathbf{K}_0$, shear modulus $\boldsymbol{\mu}_0$ and density $\boldsymbol{\rho}_0$. Because resistivity in the seawater and in the overburden and bedrock also affects estimates of reservoir parameters, we also consider the overlying resistivity model as unknown in this model and denote it by the vector $\mathbf{r}_0$, which contains the resistivity values at a small number of depths above the target zone.

We generalize the Bayesian model developed by Chen *et al.* (2007) by considering the inverted reservoir geophysical properties, such as reservoir elastic bulk modulus **K**, shear modulus $\boldsymbol{\mu}$, density $\boldsymbol{\rho}$ and electrical resistivity **r** to be random variables. Let the matrix **R** represent seismic AVA data, which are functions of elastic properties in the reservoir (i.e., **K**, $\boldsymbol{\mu}$ and $\boldsymbol{\rho}$) and in the zones outside the reservoir (i.e., $\mathbf{K}_0$, $\boldsymbol{\mu}_0$, $\boldsymbol{\rho}_0$). Let the matrix **E** represent CSEM data, which are functions of reservoir resistivity **r** and resistivity $\mathbf{r}_0$ in the seawater, the overburden and the rock beneath the reservoir (to a depth depending on skin depth). Since seismic AVA and CSEM data are two

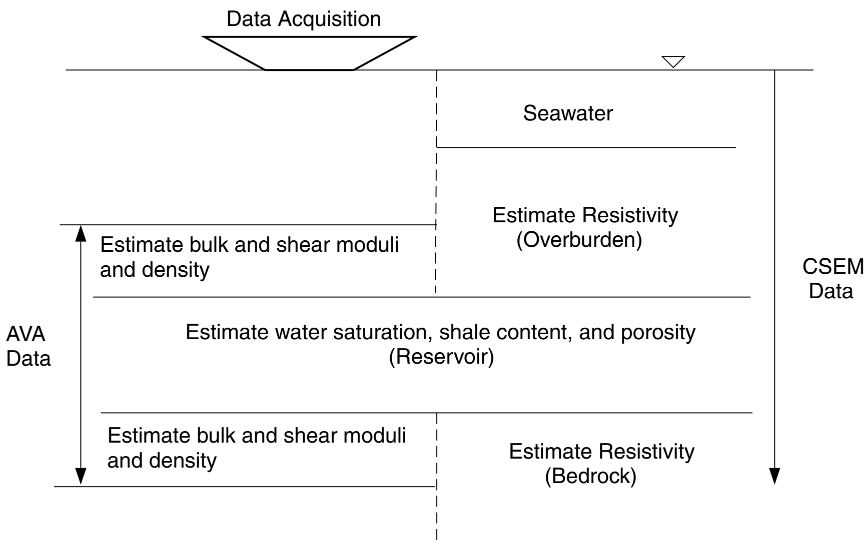

Figure 4 A schematic depiction of a layered reservoir.

different types of geophysical measurements, we assume that they are independent of each other. Consequently, we obtain the following Bayesian model:

$$\begin{aligned} &f(\mathbf{S}_w, \mathbf{c}, \boldsymbol{\phi}, \mathbf{K}, \boldsymbol{\mu}, \boldsymbol{\rho}, \mathbf{K}_0, \boldsymbol{\mu}_0, \boldsymbol{\rho}_0, \mathbf{r}, \mathbf{r}_0, \boldsymbol{\theta}_1, \boldsymbol{\theta}_2 \mid \mathbf{R}, \mathbf{E}) \propto \\ &\quad f(\mathbf{R} \mid \mathbf{K}, \boldsymbol{\mu}, \boldsymbol{\rho}, \mathbf{K}_0, \boldsymbol{\mu}_0, \boldsymbol{\rho}_0)\, f(\mathbf{E} \mid \mathbf{r}, \mathbf{r}_0) \\ &\quad f(\mathbf{r} \mid \mathbf{S}_w, \boldsymbol{\phi}, \mathbf{c}, \boldsymbol{\theta}_1)\, f(\mathbf{K}, \boldsymbol{\mu}, \boldsymbol{\rho} \mid \mathbf{S}_w, \boldsymbol{\phi}, \mathbf{c}, \boldsymbol{\theta}_2) \\ &\quad f(\mathbf{S}_w, \mathbf{c}, \boldsymbol{\phi}, \mathbf{K}_0, \boldsymbol{\mu}_0, \boldsymbol{\rho}_0, \mathbf{r}_0, \boldsymbol{\theta}_1, \boldsymbol{\theta}_2) \end{aligned} \quad . \qquad (6)$$

Equation (6) defines a joint posterior probability distribution function of all unknown parameters, which is known up to a normalizing constant. The first and second terms on the right side of the equation are the likelihood functions of seismic AVA and CSEM data, respectively. The third and fourth terms on the right side of the equation are the conditional probability distribution functions given reservoir parameters and rock-physics model parameters, which are new terms compared to the model presented by Chen *et al.* (2007) and are given by equations (2) and (5), respectively. The last term on the right side of the equation is the prior distribution of the unknown variables, which parameterize the reservoir and surrounding medium and the rock-physics models.

Likelihood models

The likelihood functions for seismic AVA and CSEM data in this study are similar to the ones used by Chen *et al.* (2007), with differences in the input of each likelihood function. Seismic reflectivity is a function of the elastic properties in the reservoir and in the zones outside the reservoir and is calculated using the Zoeppritz equations (Zoeppritz 1919) in this study. The seismic data are modelled by convolving the reflectivity with a Ricker wavelet of a given frequency and they are functions of time and incidence angle. Let the seismic data matrix be $\mathbf{R} = \{r_{ij}\}$, where $i = 1, 2, \cdots, m_t$ (m_t is the number of time samples) and $j = 1, 2, \cdots, m_a$ (m_a is the number of incidence angles). Then,

$$r_{ij} = M^a_{ij}(\mathbf{K}, \boldsymbol{\mu}, \boldsymbol{\rho}, \mathbf{K}_0, \boldsymbol{\mu}_0, \boldsymbol{\rho}_0) + \varepsilon^a_{ij}, \qquad (7)$$

where $M^a{}_{ij}$ is the $ij - th$ component of the seismic AVA forward model and $\varepsilon^a{}_{ij}$ is the corresponding measurement error. Let $\varepsilon = (\varepsilon^a_{11}, \varepsilon^a_{21}, \cdots, \varepsilon^a_{m_t 1}, \varepsilon^a_{12}, \varepsilon^a_{22} \cdots, \varepsilon^a_{m_t 2}, \cdots, \varepsilon^a_{m_t m_a})^T$ be a vector representing all the measurement errors. Let $n = m_a m_t$ be the total number of seismic data measurements in a given time window. In order to model the correlation of the measurement errors in time and across incidence angle, we assume that they are described by a multivariate Gaussian distribution with zero mean and covariance matrix $\boldsymbol{\Sigma}$, as used by Buland and Omre (2003). Consequently, we write the likelihood function for the seismic data as follows:

$$f(\mathbf{R}|\mathbf{K}, \boldsymbol{\mu}, \boldsymbol{\rho}, \mathbf{K}_0, \boldsymbol{\mu}_0, \boldsymbol{\rho}_0) = \frac{1}{\sqrt{(2\pi)^n\,|\boldsymbol{\Sigma}|}} \exp\left(-\frac{1}{2}\varepsilon^T \boldsymbol{\Sigma}^{-1} \varepsilon\right), \qquad (8)$$

where $|\boldsymbol{\Sigma}|$ and $\boldsymbol{\Sigma}^{-1}$ denote the determinant and the inverse of the covariance matrix $\boldsymbol{\Sigma}$, respectively.

The likelihood function for CSEM data is developed by considering the real and imaginary components of the recorded electric (and possibly magnetic; however, we have used only electric field data in this study) fields as data, which are collected at various offsets for different frequencies. These data are functions of electrical resistivity, which is a function of depth. Let the CSEM data matrix be $\mathbf{E} = \{e_{ijk}\}$, where $i = 1, 2, \cdots, n_f$ represents different frequencies of the CSEM sources, $j = 1, 2, \cdots, n_o$ represents different offsets and $k = 1, 2$ represents the real and quadrature components of the recorded electric field. Thus,

$$e_{ijk} = M^e_{ijk}(\mathbf{r}, \mathbf{r}_0) + \varepsilon^e_{ijk}, \tag{9}$$

where M^e_{ijk} is the $ijk - th$ component of the CSEM forward model and ε^e_{ijk} is the corresponding measurement error. Unlike for the seismic AVA data, we consider only uncorrelated electrical noise in this study. We assume that the errors in the CSEM data are proportional to the corresponding measured values with a random ratio ε^r_{ijk}, i.e., $\varepsilon^e_{ijk} = \varepsilon^r_{ijk} e_{ijk}$. We assume that the relative ratio ε^r_{ijk} has a Gaussian distribution with zero mean and standard deviation β_j that is specified and may depend on offset, typically increasing from near to far offset, for example, from 3 to 5 percent. As a result, we obtain the following likelihood function for CSEM data:

$$f(\mathbf{E} \mid \mathbf{r}, \mathbf{r}_0) = \prod_{i=1}^{n_f} \prod_{j=1}^{n_o} \prod_{k=1}^{2} \frac{1}{\sqrt{2\pi\beta_j^2}} \times \exp\left\{ -\frac{1}{2\beta_j^2} \left(\frac{e_{ijk} - M^e_{ijk}(\mathbf{r}, \mathbf{r}_0)}{e_{ijk}} \right)^2 \right\}. \tag{10}$$

We couple seismic AVA data with CSEM data by assuming the presumed reservoir has fixed boundaries in depth as shown in Fig. 4. We also assume that the depth interval of interest is common to both seismic AVA and CSEM calculations, as considered by Hoversten *et al.* (2006) and Hou *et al.* (2006). These assumptions can be removed if we consider the layer thickness or location of the reservoir as unknowns and use, for example, traveltime information to invert for their positions, but this is not the focus of this study. With the given common layer thickness and the rock-physics models presented in the second section, we can jointly invert the seismic AVA and CSEM data for unknown reservoir parameters.

Prior models

The prior distribution is determined according to several reasonable assumptions of independence among the unknown variables. For example, we assume that the unknown reservoir parameters $\mathbf{S}_w$, ϕ and $\mathbf{c}$ are independent of the unknown variables $\mathbf{K}_0$, $\boldsymbol{\mu}_0$ and $\boldsymbol{\rho}_0$ in the layers outside the reservoir, while realizing that in some geophysical situations these properties could be correlated to some extent. We also assume that water saturation $\mathbf{S}_w$ is independent of porosity ϕ and shale content $\mathbf{c}$ and that porosity ϕ is independent of shale content $\mathbf{c}$. We further assume that the electrical resistivity $\mathbf{r}_0$ in the overburden and sub-reservoir rock is independent of the elastic properties $\mathbf{K}_0$, $\boldsymbol{\mu}_0$ and $\boldsymbol{\rho}_0$ in the thin layers above and beneath the reservoir. We assume that the elastic properties $\mathbf{K}_0$, $\boldsymbol{\mu}_0$ and $\boldsymbol{\rho}_0$ are independent of each other. Finally, we assume that the unknown rock-physics model parameters $\boldsymbol{\theta}_1$ and $\boldsymbol{\theta}_2$ are independent of all the other parameters. Consequently, we can simplify the prior distribution function as:

$$f(\mathbf{S}_w, \varphi, \mathbf{c}, \mathbf{K}_0, \boldsymbol{\mu}_0, \boldsymbol{\rho}_0, \mathbf{r}_0, \boldsymbol{\theta}_1, \boldsymbol{\theta}_2) = f(\mathbf{S}_w) f(\varphi) f(\mathbf{c}) f(\mathbf{K}_0) f(\boldsymbol{\mu}_0) f(\boldsymbol{\rho}_0) f(\mathbf{r}_0) f(\boldsymbol{\theta}_1) f(\boldsymbol{\theta}_2). \tag{11}$$

We assume that the prior distribution of each unknown parameter in equation (11) is given by a uniform probability distribution with a specified range. For the synthetic study presented in the fourth section, the prior ranges of water saturation, porosity and shale content are given by (0, 1), (0.01, 0.4) and (0, 1), respectively. The prior ranges of elastic moduli and density and overburden resistivity are given by the lower and upper bounds that are 5% away from their corresponding true values. The prior ranges of the rock-physics model parameters are determined by the given coefficients of variation, which vary among the case studies that we present.

Sampling methods

We use Markov chain Monte Carlo sampling methods to explore the joint posterior probability distribution function described by equation (6). Similar to the sampling strategies used by Chen *et al.* (2007), we adopt a mixed sampling method as advocated by Tierney (1994), which includes single-variable Metropolis-Hastings methods (Metropolis *et al.* 1953; Hastings 1970), multivariate Metropolis-Hastings methods, single-variable slice sampling methods (Neal 2003) and multivariate slice sampling methods. At each sampling step, we randomly pick one of the above four methods. This strategy has been shown to be very efficient for solving this type of joint inversion problem.

SYNTHETIC CASE STUDY

In this section, we investigate the effects of uncertainty and biases in rock-physics models on the estimates of reservoir parameters by applying the developed Bayesian model to a synthetic layered reservoir, built according to a typical deep-water clastic geophysical scenario, such as might be encountered in the Gulf of Mexico or in offshore West Africa. We primarily compare the estimates of reservoir parameters when uncertainty and biases are incorporated into the joint inversion with those when uncertainty and biases are not fully taken account in the estimation, as is done in conventional inversion approaches. Since our purpose in this study is to investigate the effect of uncertainty in rock-physics models, we keep the synthetic model simple while using model parameters that are representative of those found in actual clastic reservoirs in sedimentary basins.

Synthetic true model

The synthetic model includes an oil reservoir embedded in a shale package. The reservoir is assumed to consist of one layer with a thickness of 50 m and with shale content c, porosity ϕ and water saturation S_w of 0.1, 0.32 and 0.1, respectively. Figure 5 shows the vertical profiles of water saturation, shale content and porosity from the water surface to a depth of 4000 m, with the seafloor located at 1120 m from the water surface. The water saturation and shale content in the rock beneath the seafloor are constant (100%), while porosity varies with depth, except in the oil reservoir, where both water saturation and shale content are equal to 0.1 and porosity is equal to 0.32.

The synthetic seismic amplitude variation with angle (AVA) data are normal-moveout corrected angle gathers that are generated by convolving a 25 Hz Ricker wavelet with the angle-dependent reflectivity, which is calculated using the Zoeppritz equations (Zoeppritz 1919) for each layer interface. Figure 6 shows the synthetic seismic AVA data without noise. The vertical resolution of seismic data is a function of wavelength and it is about 15 m for the synthetic study, which is smaller than the thickness of the reservoir layer. The seismic traces are calculated for seven incidence angles (5, 10, 15, 20, 25, 30 and 35 degrees) and are sampled at 2 ms. In reality, the seismic AVA data are extracted from a predetermined time window that covers the depth interval of interest and that is determined from check shots or from calculations of time-depth pairs (Chen *et al.* 2007). To account for uncertainty in choosing the time window, we add two 50 m thick layers above the reservoir layer and one 50 m thick layer below the reservoir layer.

The marine controlled-source electromagnetics (CSEM) data consist of the electric fields measured at six receivers deployed on the seafloor from a ship-towed electric dipole source at five different frequencies (0.10, 0.25, 0.50, 0.75 and 1.00 Hz). The six source-receiver offsets are 4, 5, 6, 7, 8 and 10 km, respectively. Figure 7 shows the amplitudes and phases of recorded electric fields with offsets from 4,000 m to

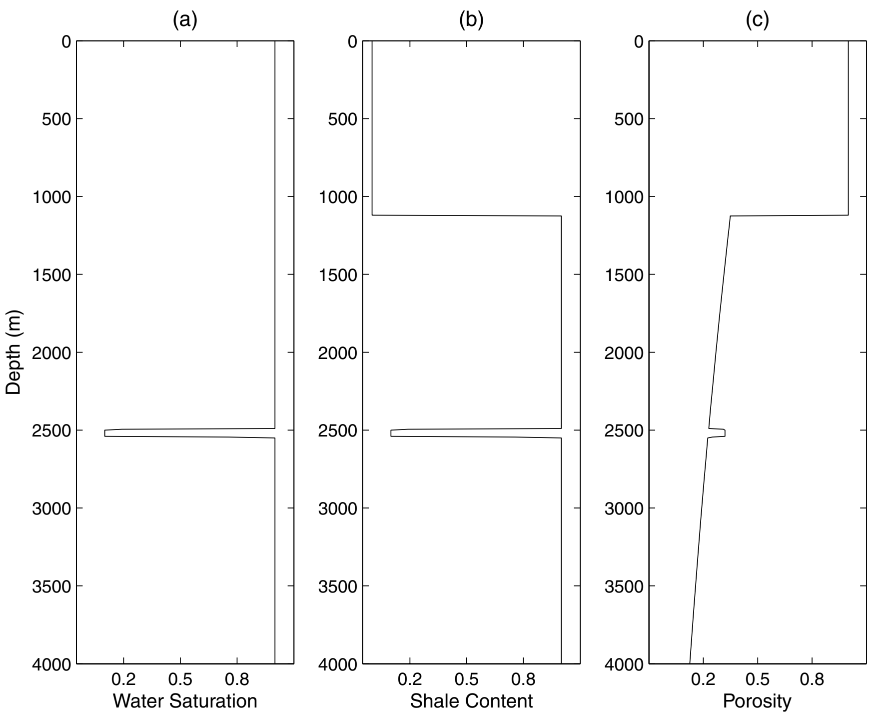

Figure 5 Vertical profiles of water saturation (a), shale content (b) and porosity (c) for the synthetic case study.

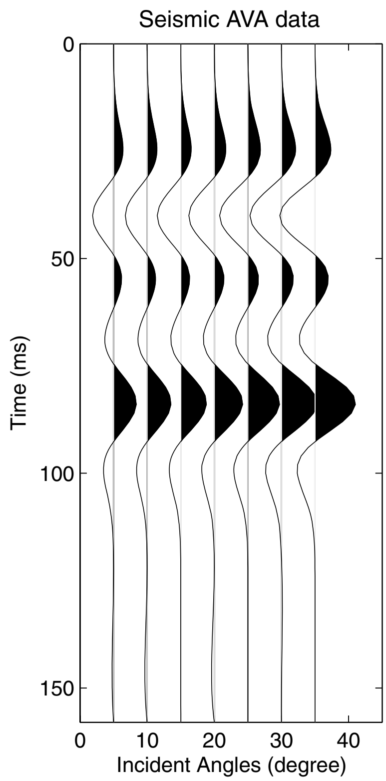

Figure 6 Synthetic seismic AVA data without noise.

10,000 m for frequencies of 0.25 Hz, 0.5 Hz and 0.75 Hz. The spatial resolution of CSEM data is significantly lower than that of seismic AVA data. Unlike seismic data where the vertical resolution is proportional to seismic wavelength, the spatial resolution of the electromagnetic data is mainly limited by the noise level in the data and by the source-receiver spacing (Hesthammer and Boulaenko 2005; Hokstad and Rosen 2007). With the use of the synthetic seismic and CSEM data, a thickness of 50 m for the reservoir layer seems to be a reasonable choice for the joint inversion which was also used by Hesthammer and Boulaenko (2005) in their real case study. Because CSEM data are sensitive to the resistivity profile to a depth of several skin depths (i.e., a few thousands of metres), in order to account for the effects of electrical resistivity in the overburden and bedrock on the recorded CSEM data, we divide the overburden into five layers. We jointly invert the resistivity in the five overburden layers and in the bedrock.

Since our focus in this study is on the effects of uncertainty and bias in rock-physics models, we invert the true seismic AVA and CSEM data in the subsequent case studies, although we assume that the generated synthetic data include various levels of noise. This is because inverting data with actual noise added may lead to results that depart from the true models due to conditioning on the specific noise realization utilized in the inversion. We assume that the synthetic seismic data include spatially correlated Gaussian random noise and that the spatial correlation of the noise is determined by an exponential variogram with an integral length of 2 ms. The variance of the Gaussian noise is angle dependent, with signal-to-noise ratios of 12, 11, 10, 9, 8, 7 and 5 from the near to the far offset. For the CSEM data, we assume relative noise levels that increase from 3 to 5% from the near to the far offset. We did not put a relative weight between the seismic and CSEM data as done by deterministic inversion methods, which is

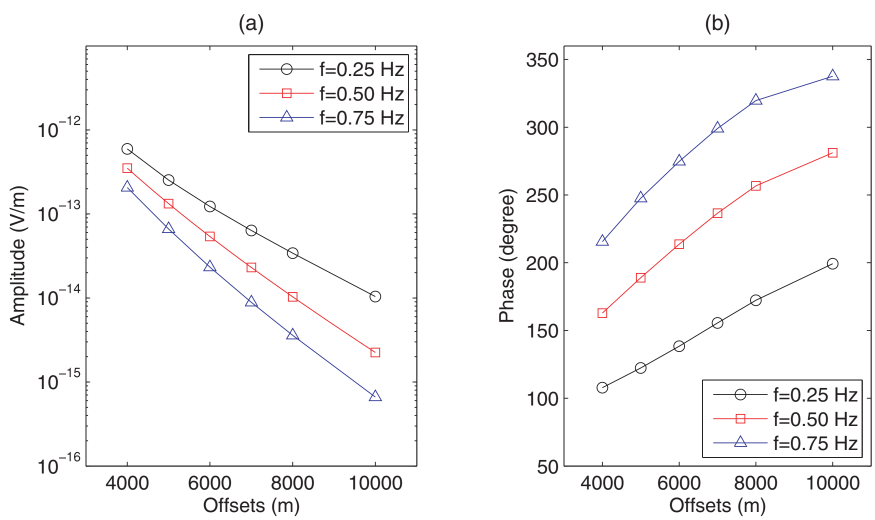

Figure 7 Synthetic CSEM data at the frequencies of 0.25 Hz, 0.50 Hz and 0.75 Hz.

implicitly carried out by the errors in seismic and CSEM data in this study.

Uncertainty in rock-physics model predictions

We vary the additive errors in the outputs of the rock-physics models by specifying various levels of the coefficient of variation. Figure 8 shows the estimated marginal posterior probability density functions of the inverted water saturation, shale content and porosity using synthetic seismic AVA and CSEM data when the predictions of the rock-physics models contain various levels of uncertainty. The black, red, blue and green curves are the estimated posterior probability density functions when the rock-physics models are exact or have errors equal to the coefficients of variation of 1, 3 and 5%, respectively. The black triangles are the true values of water saturation, shale content and porosity. Comparison of the estimated marginal probability density functions to the corresponding true values shows that uncertainty in the outputs of rock-physics models has a significant effect on the estimates of reservoir parameters. As the coefficients of variation increase, the spread of the estimated probability density functions increases and the medians of the estimated probability density functions of shale content and porosity shift toward the centre of each prior range (0.5 for shale content and 0.2 for porosity). From the figure, we also note that the estimate of water saturation is much less sensitive to uncertainty in the outputs of the rock-physics models compared to shale content and porosity.

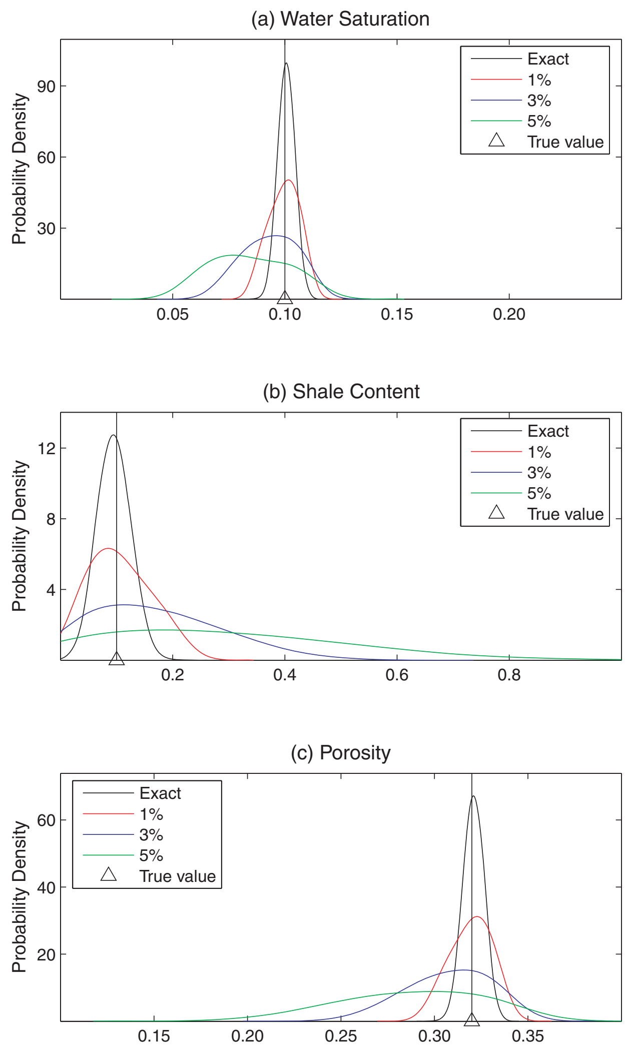

Figure 8 Estimated marginal posterior probability density functions of water saturation, shale content and porosity, where the black, red, blue and green curves are the estimated posterior probability density functions when the predictions of the rock-physics models are exact or have errors equivalent to coefficients of variation of 1, 3 and 5%, respectively.

Uncertainty in rock-physics model parameters

Uncertainty in rock-physics model parameters is often underestimated or ignored in conventional approaches for geophysical inversion due to the difficulty of incorporating it into the estimation. The Bayesian model developed in this paper provides a general framework for investigating different sources of uncertainty simultaneously. To compare with the effects of uncertainty in rock-physics model predictions, we also use the coefficient of variation to measure uncertainty in rock-physics model parameters. Let (a, b) be the interval on which the rock-physics model parameter θ is uniformly distributed. Let q be the coefficient of variation of the parameter θ. The mean and variance of the variable are given by $(a+b)/2 = \theta$ and $(b-a)^2/12 = (q\theta)^2$, respectively. By solving the above two equations, we obtain $a = (1-\sqrt{3}q)\theta$ and $b = (1+\sqrt{3}q)\theta$.

Figure 9 compares the estimated marginal posterior probability density functions of the inverted water saturation, shale content and porosity when the rock-physics model parameters are exact or have errors equivalent to the coefficients of variation of 1, 3 and 5%. In this case, we assume that the outputs of the rock-physics models do not include any additive errors. Like uncertainty in the predictions of the rock-physics models, uncertainty in the model parameters also affects the estimates of reservoir parameters significantly. Again, water saturation is less sensitive to uncertainty in the model parameters than shale content and porosity and the distribution widths (uncertainties) increase with the coefficients of variation of the model parameters. However, compared with uncertainty

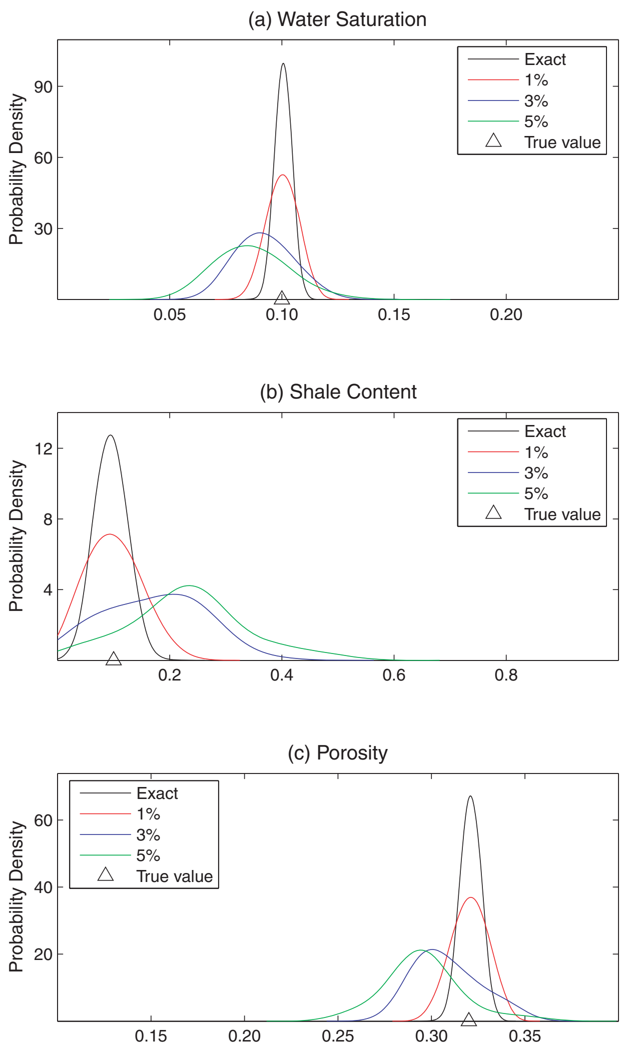

Figure 9 Estimated marginal posterior probability density functions of water saturation, shale content and porosity, where the black, red, blue and green curves are the estimated posterior probability density functions when the rock-physics model parameters are exact or have errors equivalent to coefficients of variation of 1, 3 and 5%, respectively.

in rock-physics model predictions (Figure 8), the effects of uncertainties in the model parameters are less significant, especially for the larger values of the coefficient of variation.

Biases in rock-physics models

In practice, rock-physics models may include unknown biases and they may have significant effects on the estimates of reservoir parameters in the joint inversion of seismic and CSEM data. Figure 10 shows the estimated pairwise posterior probability density functions of water saturation, shale content and porosity when the rock-physics model predictions are unbiased (black curves) or have negative biases that are equal to 1% (red curves) and 3% (blue curves) of the corresponding true model predictions. The effects of biases in the model predictions on the inverted parameters are quite complex. The estimated water saturation and porosity decrease, whereas the estimated shale content increases. Essentially, in order to be compatible with the same seismic amplitude variation with angle (AVA) and controlled-source electromagnetics (CSEM) data, the outputs of the new rock-physics models have to be increased to compensate for the reduction in reservoir geophysical attributes due to the added negative biases.

Biases in rock-physics model parameters

Similarly, the parameters associated with rock-physics models may also suffer from unknown biases and they may have important effects on reservoir parameter estimation. Figure 11 shows the estimated pairwise posterior probability density functions of water saturation, shale content and porosity when the model parameters are unbiased or have biases equal to 1 and 3% of the corresponding true values. Again, the estimated reservoir parameters shift. The water saturation and porosity increase but the estimated shale content decreases. Note that the introduction of biases does not necessarily lead to appreciable spreading of the posterior probability distributions. Therefore, it could be difficult to diagnose the presence of such biases in the rock-physics models by examining the inversion results.

DISCUSSION AND CONCLUSIONS

We have developed a Bayesian model to investigate the effects of uncertainty in rock-physics models on reservoir parameter estimation and have applied it to a synthetic layered reservoir. The results of the case study show that uncertainty in both the outputs and the parameters of rock-physics models may have significant effects on the estimates of reservoir parameters when we jointly invert seismic AVA and CSEM data. While it is certainly clear that model uncertainties would lead to a reduction of the reliability of parameter estimation, our method provides a means of studying the magnitude of these errors quantitatively. Generally, the effects of uncertainty in rock-physics model parameters are less significant than those of uncertainty in rock-physics model predictions.

Note that in our synthetic case study, we investigate the effects of uncertainty in rock-physics model predictions and in

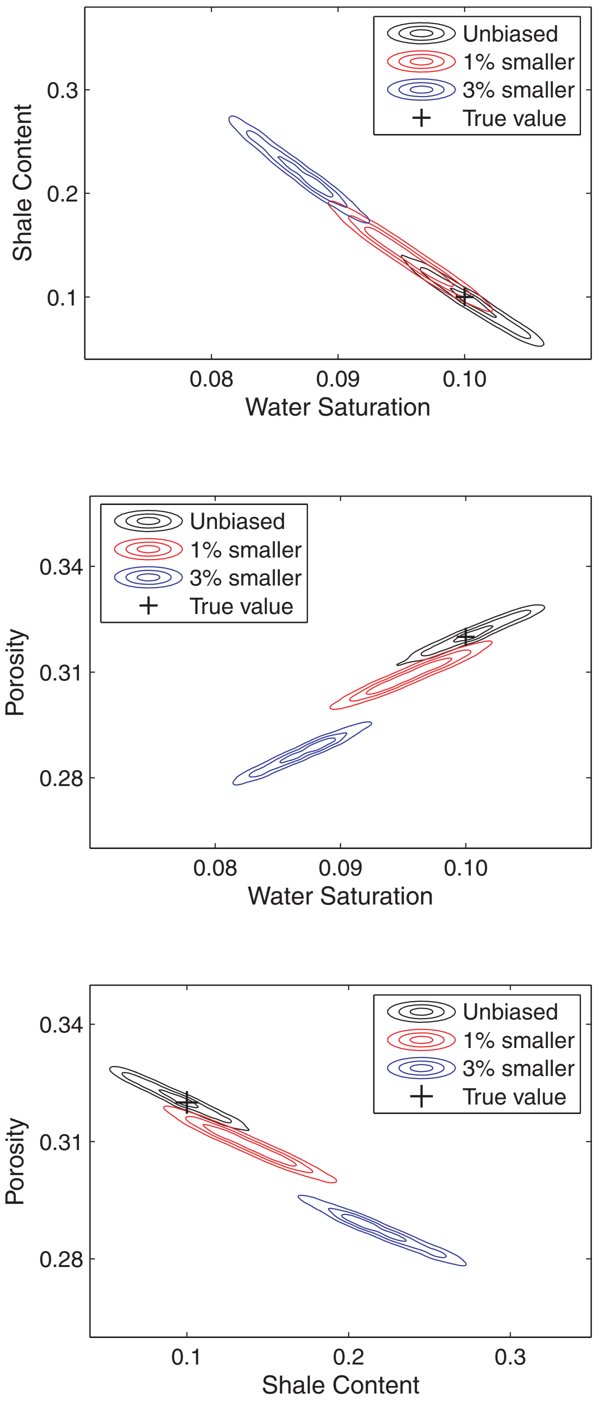

Figure 10 Contours of the estimated pairwise posterior probability density functions of water saturation, shale content and porosity when the predictions of the rock-physics models are unbiased (black curves) or have negative biases that are equal to 1% (red curves) and 3% (blue curves) of their corresponding true values.

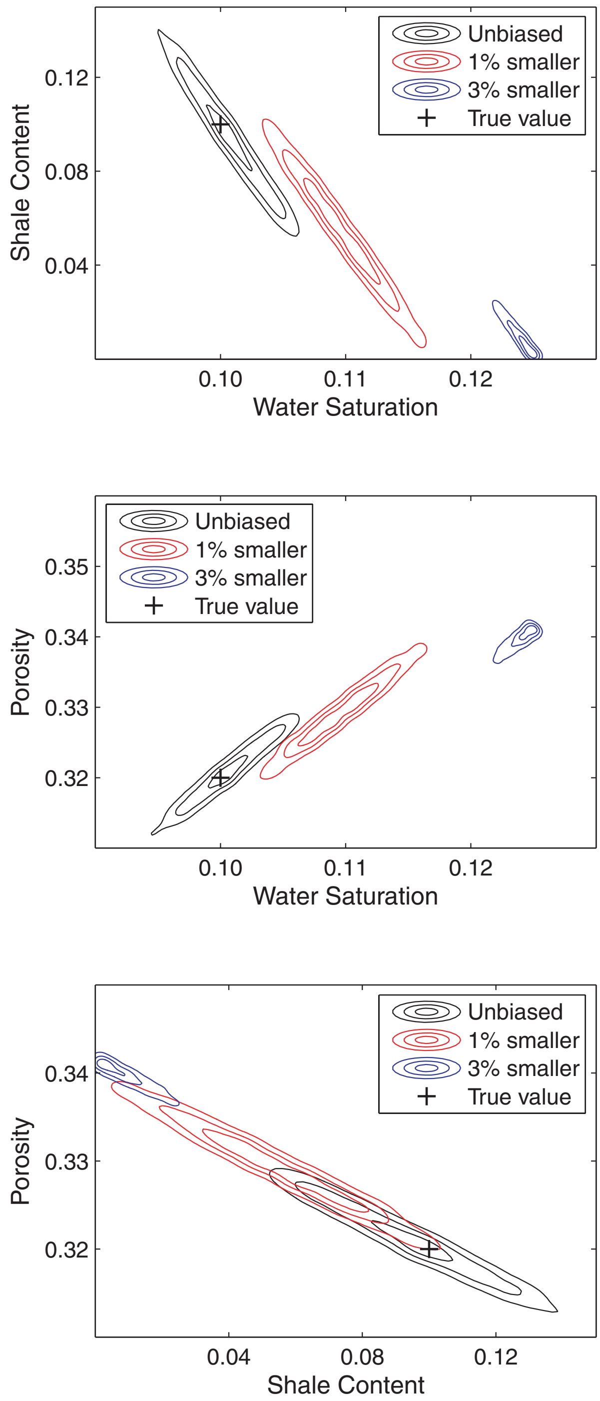

Figure 11 Contours of the estimated pairwise posterior probability density functions of water saturation, shale content and porosity when the parameters of the rock-physics models are unbiased (black curves) or have negative biases that are equal to 1% (red curves) and 3% (blue curves) of their corresponding true values.

their associated parameters separately. In practice, they may be and are likely to be, present together and their compound effects on the estimates of reservoir parameters typically are not more than the simple summation of the effects caused by the two different types of uncertainty. However, as shown in the synthetic study, totally ignoring uncertainty in rock-physics model predictions, in their associated parameters, or in both quantities, will very likely lead to over-optimistic estimates of the reliability of inverted reservoir parameters. Additionally, we assign the same levels of uncertainty to all the outputs and the parameters of rock-physics models. In reality, some model predictions or some model parameters may be subject to larger degrees of uncertainty than others and their assembled effects could be worse than what we have shown in the synthetic case study. This poses another risk when the uncertainty in rock-physics models is not taken into consideration in the joint inversion.

We have also demonstrated the effects of biases in rock-physics models on the estimates of reservoir parameters. As shown in the synthetic study, unknown biases in both rock-physics model predictions and in the model parameters will result in very misleading results for the joint inversion. For instance, the modes or the medians of the estimated posterior probability density functions of reservoir parameters are shifted away from their corresponding true values, as derived when we assume that the outputs and the parameters of rock-physics models are exact. In addition, since the unknown biases do not tend to induce a widening of the posterior probability distribution functions, we may not be able to find the existence of such biases in the rock physics models by examining the inversion results.

The main goal of this study is to demonstrate the effects of uncertainty in rock-physics models on reservoir parameter estimation in joint inversion of seismic AVA and CSEM data and to raise awareness about those effects in the joint inversion. Notice that the case study represented in this work is an ideal case for reservoir parameter estimation, where we assume that the seismic waveforms and the location of the target reservoir can be estimated reasonably well. However, in practice, the joint inversion may be subject to the effects of many other uncertainties, such as errors in data acquisition and processing, scale discrepancies between seismic AVA and CSEM data, errors in estimation of seismic waveforms, errors in locations of target reservoirs, etc. The relative effects of uncertainty in rock-physics models on reservoir parameter estimation compared to uncertainties in other sources associated with the joint inversion depend on the specific problem. To evaluate the assembled or compounding effects of those uncertainties, an integrated approach is needed. The Markov chain Monte Carlo sampling based Bayesian model developed in this study provides a general framework for taking into account various sources of uncertainty simultaneously in the joint inversion.

ACKNOWLEDGEMENTS

This work was funded by ExxonMobil Upstream Research Company. We thank Shiyu Xu for providing his rock-physics model codes and for advice on selecting parameters for our synthetic models.

REFERENCES

Archie G.E. 1942. The electrical resistivity log as an aid in determining some reservoir characteristics. *Transactions of the American Institute of Mechanical Engineers* **146**, 54–62.

Bachrach R. 2006. Joint estimation of porosity and saturation using stochastic rock-physics modelling. *Geophysics* **71**, O53–O63.

Buland A. and Omre H. 2003. Bayesian linearized AVO inversion. *Geophysics* **68**, 185–198.

Cadigan N.G. and Myers R.A. 2001. A comparison of Gamma and Lognormal maximum likelihood estimators in a sequential population analysis. *Canadian Journal of Fisheries and Aquatic Sciences* **58**, 560–567.

Chen J., Hoversten M., Vasco D., Rubin Y. and Hou Z. 2007. A Bayesian model for gas saturation estimation using marine seismic AVA and CSEM data. *Geophysics* **72**, WA85–WA95.

Dvorkin J. and Nur A. 1996. Elasticity of high-porosity sandstones: Theory for two North Sea datasets. *Geophysics* **61**, 1363–1370.

Firth D. 1988. Multiplicative errors: Lognormal or Gamma. *Journal of the Royal Statistical Society, Series B* **50**, 266–268.

Gassmann F. 1951. Elastic waves through a packing of spheres. *Geophysics* **16**, 673–685.

Hastings W.K. 1970. Monte Carlo sampling methods using Markov chains and their applications. *Biometrika* **57**, 97–109.

Hesthammer J. and Boulaenko M. 2005. The offshore EM challenge. *First Break* **23**, 59–66.

Hokstad K. and Rosen T. 2007. On the relationship between depth migration of controlled-source electromagnetic and seismic data. *The Leading Edge* **26**, 342–354.

Hou Z., Rubin Y., Hoversten G.M., Vasco D. and Chen J. 2006. Reservoir-parameter identification using minimum relative entropy-based Bayesian inversion of seismic AVA and marine CSEM data. *Geophysics* **71**, O77–O88.

Hoversten G., Cassassuce F., Gasperikova E., Newman G., Chen J., Vasco D. *et al.* 2006. Direct reservoir parameter estimation using joint inversion of marine seismic AVA and CSEM data. *Geophysics* **71**, C1–C13.

Kuster G.T. and Toksöz M.N. 1974. Velocity and attenuation of seismic waves in two phase media: Theoretical formulations. *Geophysics* **39**, 587–606.

Mavko G., Mukerji T. and Dvorkin J. 1998. *The Rock Physics Handbook: Tools for Seismic Analysis in Porous Media*. Cambridge University Press.

Metropolis N., Rosenbluth A.W., Rosenbluth M.N., Teller A.H. and Teller E. 1953. Equations of state calculations by fast computing machines. *Journal of Chemical Physics* **21**, 1087–1092.

Neal R.M. 2003. Slice sampling. *Annuals of Statistics* **31**, 705–767.

Norris A.N. 1985. A differential scheme for the effective moduli of composites. *Mechanics of Materials* **4**, 1–16.

Poupon A. and Leveaux J. 1971. Evaluation of water saturation in shaley formations. 12th Annual Society of Professional Well Log Analysts Logging Symposium Transactions, 1–2.

Poupon A., Loy M.E. and Tixier M.P. 1954. A contribution to electrical log interpretation in shaley sands. *Transactions of the American Institute of Mining Engineers* **201**, 138–145.

Tierney L. 1994. Markov chains for exploring posterior distributions. *Annals of Statistics* **22**, 1701–1762.

Xu S. and White R.E. 1995. A new velocity model for clay-sand mixture. *Geophysical Prospecting* **43**, 91–118.

Zoeppritz K. 1919. Erdbebenwellen VIII B. On the reflection and propagation of seismic waves. *Göttinger Nachrichten* **1**, 66–84.